J Mol Med
DOI 10.1007/s00109-014-1201-y

JMolMed

ORIGINAL ARTICLE

Activation of the stress response in macrophages alters the M1/M2 balance by enhancing bacterial killing and IL-10 expression

Virginia L. Vega · Laura E. Crotty Alexander · Wisler Charles · John H. Hwang · Victor Nizet · Antonio De Maio

Received: 8 October 2013 / Revised: 12 July 2014 / Accepted: 21 July 2014

Abstract
Macrophages (Mϕs) play an important role in the inflammatory response during injury by participating in the removal of injurious stimuli, such as bacteria, and promoting tissue healing to restore homeostasis. Mϕs can acquire distinct functional phenotypes along a spectrum between two opposite stages (M1/M2) during activation. In the present study, we induced a stress response in Mϕs via heat shock (HS) and found that it incurred an increase in phagocytosis (1.6-fold, $P<0.05$) and bacterial killing (2.8-fold, $P<0.01$). Upon heat stress activation, Mϕs respond to group B *Streptococcus* (GBS) infection with lower levels of pro-inflammatory cytokines, TNF-α (2.25-fold, $P<0.01$), IL-6 (7-fold, $P<0.001$), and inducible nitric oxide synthase (iNOS) (2.22-fold, $P<0.05$), but higher levels of the anti-inflammatory cytokine IL-10 (3.9-fold, $P<0.01$). Stressed Mϕs exposed to GBS display rapid phagosome maturation, increased extracellular trap (ET) formation and elevated cathelicidin antimicrobial peptide expression (2.5-fold, $P<0.001$). These findings are consistent with a heretofore uncharacterized Mϕ activation state formed in response to stress, associated with secretion of large quantities of anti-inflammatory mediators and redirection of antimicrobial mechanisms to NADPH-oxidase-independent pathways. This "friendly activation" of Mϕs is characterized by increased bactericidal activity and more rapid and controlled resolution of the inflammatory response.

V. L. Vega and L. E. Crotty Alexander contributed equally to this work

Electronic supplementary material The online version of this article (doi:10.1007/s00109-014-1201-y) contains supplementary material, which is available to authorized users.

V. L. Vega
Research and Development Division, SkinMedica, Inc., Carlsbad, CA 92008, USA

L. E. Crotty Alexander · J. H. Hwang
Pulmonary and Critical Care Section, VA San Diego Healthcare System, La Jolla, CA 92093, USA

L. E. Crotty Alexander · J. H. Hwang
Division of Pulmonary and Critical Care, School of Medicine, University of California San Diego (UCSD), La Jolla, CA 92093, USA

W. Charles
Initiative for Maximizing Student Development, UCSD, La Jolla, CA 92093, USA

V. Nizet
Department of Pediatrics, School of Medicine, UCSD, La Jolla, CA 92093, USA

V. Nizet
Division of Pediatric Pharmacology and Drug Discovery, Skaggs School of Pharmacy, UCSD, La Jolla, CA 92093, USA

A. De Maio
Departments of Surgery and Neurosciences, School of Medicine, UCSD, La Jolla, CA 92093, USA

A. De Maio
Center for Investigations of Health and Education Disparities, UCSD, La Jolla, CA 92093, USA

A. De Maio (✉)
University of California San Diego, 9500 Gilman Drive, #0739, La Jolla, CA 92093-0739, USA
e-mail: ademaio@ucsd.edu

Published online: 28 August 2014

Key Messages

- Macrophages form a dual pro-bactericidal and anti-inflammatory state.
- Stress in the setting of infection triggers friendly activation in macrophages.
- Heat shock plus infection increases macrophage bactericidal activity.
- Heat shock plus infection increases macrophage extracellular trap formation.
- Heat shock plus infection increases macrophage production of cathelicidin and IL-10.

Keywords Macrophage activation · Heat shock · Macrophage phenotype and functional polarization · Stress response · Group B Streptococcus · Macrophage extracellular traps

Introduction

Inflammation is a natural response to infection and tissue damage directed at protecting the individual by removing pathogens and injurious stimuli and through facilitating tissue repair. However, elevated or sustained inflammatory responses are detrimental and have been associated with a large number of disorders, including atherosclerotic heart disease, asthma, chronic obstructive pulmonary disease, autoimmunity, sepsis, inflammatory bowel disease, allergies, and genetic or acquired immunodeficiency [1]. The mechanisms that control inflammation are incompletely understood. Therefore, few targeted therapeutic options are available to modulate aberrant inflammatory processes [2–4]. Macrophages (Mϕs) are key host cells involved in the initiation and orchestration of inflammatory responses. Mϕ activation results in reversible functional polarization, progressing from M1 (pro-inflammatory) to M2 (anti-inflammatory or regulatory) phenotypes with the development of several intermediary stages in between [5–9]. An adequate and time-appropriate Mϕ functional phenotype switch can mitigate the progression of inflammatory diseases [10–12]. Consequently, a better understanding of the factors that control Mϕ switching between phenotypes may provide therapeutic or pharmacological options for the treatment of diverse pathologies.

One main function of Mϕs is the removal of pathogens and damaged cells, which commonly results in parenchymal tissue damage due to the production of pro-inflammatory factors [13]. Upon activation with pro-inflammatory agents, such as M1 ligands (e.g., bacterial components), Mϕs undergo a series of physiologic changes that result in the activation of killing mechanisms as well as the secretion of a large number of pro- and anti-inflammatory mediators that modulate Mϕ function, control the recruitment and activation of other inflammatory cells, and alter cell metabolism [14]. We have previously shown that activation of the stress response (SR), a common cellular defense mechanism against a variety of insults, significantly modulates Mϕ responses to M1 ligands [15, 16], resulting in more efficient clearance of pathogens and cell debris. The mechanisms involved in this SR-associated improvement in Mϕ function are unknown, but they are likely linked to the upregulation of heat shock proteins (Hsps) [15–17].

Pathogen clearance is the result of several well-coordinated processes such as detection and binding of the pathogen, phagocytosis, phagosome maturation, targeting to lysosomes, and final destruction [18, 19]. Mϕs have several mechanisms to destroy pathogens, including the production of reactive oxygen and nitrogen species (ROS and RNS). The strong production of superoxide anion ($O_2^{\cdot-}$) observed upon pathogen recognition is due to activation and assembly of the membrane NADPH-oxidase. We have previously demonstrated a significant decrease in $O_2^{\cdot-}$ production in thermally stressed Mϕs activated with M1 ligands [15]. This finding was in agreement with other publications that additionally showed that heat shock (HS)-associated inhibition of NADPH-oxidase is not driven by heat denaturation, inhibition of protein synthesis, and changes in cytosolic pH, oxidative stress, or alterations in actin cytoskeleton functions [20–22].

In this study, we further characterize the functional changes triggered by activating the SR in Mϕs. We observe that stressed Mϕs respond to bacterial infection (classically considered an M1 stimulus or ligand) not only with elevated phagocytosis and increased bactericidal activity but also with enhanced production of anti-inflammatory mediators and elevated expression of M2 markers. These data support the formation of a new Mϕ functional phenotype in response to SR activation, which may promote faster resolution of inflammation and, therefore, accelerated restoration of homeostasis.

Materials and methods

Reagents

Alexa Fluor (AF) 488-labeled *Escherichia coli* (*E. coli*; K-12 strain), *Staphylococcus aureus* (*S. aureus*; Wood strain, lacking protein A) particles, and fluorescein (FITC)-conjugated IL-10R antibody were purchased from Molecular Probes Inc. *E. coli* (O26:B6) lipopolysaccharide (LPS) was obtained from Difco Laboratories and zymozan and PMA from Sigma-Aldrich. *Streptococcus agalactiae* strain COH1 is a highly encapsulated serotype III group B *Streptococcus* (GBS) obtained from a fatal neonatal sepsis case [23]. STAT3 antibody was kindly provided by AVIVA Systems Biology, CA. AF532-conjugated cholera toxin subunit B and AF532-transferrin were purchased from Invitrogen Life Technologies.

Animal studies

All mice, BALB/c male mice (8 weeks old), were purchased from Jackson Laboratories. Under sterile conditions alveolar (AMϕs) and peritoneal (PMϕs) were isolated by bronchoalveolar lavage and peritoneal lavage from naïve mice utilizing cold SF RPMI1640 medium, as described in detail previously [24–26]. In some studies, mice were subjected to thermal stress as previously described [27]. In brief, mice were anesthetized with ketamine 100 mg/kg i.p.; a rectal thermistor probe was inserted; and mice were warmed via heating blanket until core body temperature reached 42 °C. This temperature was maintained for 10 min and then mice were returned to their cages. Control mice were anesthetized but not subjected to thermal stress. All animal protocols were reviewed and approved by the UCSD Institutional Animal Care and Use Committee according to the National Institutes of Health guidelines.

Cell culture and heat shock induction

Mouse Mϕ cell lines (J774 and RAW264.7) and naïve alveolar macrophages (AMϕs) or peritoneal macrophages (PMϕs) isolated from BALB/c mice were cultured in RPMI 1640 medium supplemented with 10 % heat-inactivated fetal bovine serum (FBS), 10 IU/ml penicillin, and 10 μg/ml streptomycin at 37 °C with 5 % CO_2 in a humidified incubator. Cells were plated in antibiotic-free medium for at least 16 h before experiments. Heat shock (HS) was performed by incubation of cells for 1.5 h at 42 °C, followed by recovery at 37 °C.

Todd-Hewitt broth (THB) was inoculated with one colony of GBS and allowed to grow to stationary phase overnight. Two hundred microliters of GBS overnight culture was inoculated into 10 ml of fresh THB and grown to mid-log phase (abs 0.4 at 600 nm). Bacteria were spun at 4,000 rpm for 10 min and resuspended in PBS to abs 0.4 at 600 nm, giving 1×10^8 colony forming units (CFU)/ml. Bacteria were diluted 1:10 in PBS for a final concentration of 1×10^7 CFU/ml. For studies utilizing a multiplicity of infection (MOI) of 1, for every 2×10^5 macrophages, 2×10^5 CFU of GBS were used (20 μl at 1×10^7 CFU/ml). For an MOI of 0.1, 2 μl at 1×10^7 CFU/ml were used.

Phagocytosis

GBS was grown in THB (Difco) and on Todd-Hewitt agar plates at 37 °C. Mϕs were harvested by scraping and plated at 2×10^5 cells/well for 16 h prior to phagocytosis assays. Mϕs were washed twice with sterile PBS and incubated with serum-free (SF) medium for 30 min at 37 °C, followed by incubation with 50 μl AF488-bacteria particles (70 μg/ml) for 2 h at 37 °C or by incubating with live GBS-GFP at an MOI of 1 at 37 °C for 1 h [28]. Mϕs were washed twice with SF medium and PBS to remove noninternalized bacteria particles or live bacteria. To quench noninternalized signal, Mϕs were incubated with PBS pH 5.0 for 15 min, then fixed in 4 % paraformaldehyde (PFA) for 10 min. Samples to be tested for bacteria adherent to the outside of the Mϕs were not quenched prior to fixation. Slides were mounted using 3.9 % DABCO in PermaFluor aqueous mounting medium (Thermo Scientific) and visualized using confocal microscopy.

Phagosome maturation

Studies were performed as previously described by Chow et al. [29]. In brief, 2.5×10^5 J774 Mϕs were grown on round glass cover slips for 16 h as described previously [15]. At the desired time point, stressed and control Mϕs were incubated in SF medium for 1 h at 37 °C to deplete endogenous transferrin. Mϕs were then cultured in the presence of AF532-transferrin (50 μg/ml) for 30 min at 25 °C to label early/recycling endosomes (red). Noninternalized transferrin was removed by washing with PBS. AF488-bacterial particles (70 mg/ml; nonopsonized) were added for 1, 5, and 7 min at 25 °C. Maturation of phagosomes was evaluated by fluorescent microscopy as co-localization of transferrin-labeled endosomes (red) with bacteria particle containing phagosomes (green). Experiments were repeated in PMϕs. For quantifying Mϕ endocytosis of transferrin and cholera toxin, J774 Mϕs were incubated for 30 min in SF medium followed by incubation with fluorescent transferrin (50 μg/ml) or cholera toxin (5 mcg/ml) for 30 min at 37 °C. Noninternalized signal was removed by washing with PBS. Internalized signal was rectified by MTT in each well and expressed as endocytic index (intensity of the signal/MTT). Experiments were performed in triplicate and repeated at least three times.

Ratio of internalization of FITC-IgG-BSA

Mϕs were incubated with FITC-IgG-BSA at 4 °C to allow binding, but not internalization, of the complex. Mϕs were then placed at 25 °C for up to 2 h to allow internalization of the complex. Cells were washed twice with SF medium to remove unbound complex, and the noninternalized signal was quenched by incubation in PBS pH 5.0. Quantification of internalized signal was performed by fluorometry; fluorescent values were corrected to the estimated number of live cells (measured via MTT) in each well. Experiments were performed three times and statistical significance evaluated by one-way analysis of variance (ANOVA) followed by Newman-Keuls test.

qRT-PCR

One million Mϕs were subjected to HS (42 °C for 90 min) or not (37 °C) and allowed to recover for different lengths of time

up to 24 h at 37 °C. In some experiments, control and HS Mϕs were incubated with or without 100 ng/ml LPS or 200 μg/ml zymozan for 2 h, or GBS at MOI 1 for 1 h. Total mRNA was isolated using Trizol, and mRNA expression levels were evaluated by quantitative reverse transcription PCR (qRT-PCR) using commercial primers. Efficiencies of all primers were within 85–100 %. Values were rectified by GAPDH. In the case of cathelicidin-related antimicrobial peptide (CRAMP), arg-1, mrc-1, IL-4, ym-1, ym-2, and ptgs-2 relative gene expressions were calculated using ΔΔCt analysis. Results for pro- and anti-inflammatory cytokines are expressed as copies of target gene/copies of GAPDH.

Bacterial killing

Bactericidal assays were run with primary Mϕs (PMϕs) in parallel with J774 and RAW264.7 cell lines. Mϕs (1×10^5) were placed in 96-well flat-bottom plates and cultured with 50 μl of RPMI 1640 medium supplemented with 2 % FBS. Cells were allowed to adhere for 2 h at 37 °C with 5 % CO_2 and then stimulated with PMA (10 ng/ml, 30 min). To block phagocytosis, cytochalasin D (50 μM) was added 30 min prior to infection. To dissolve extracellular DNA traps, micrococcal nuclease was added at 1:500 for 20 min. Supernatant was removed and replaced with fresh RPMI 1640 media. Cells were incubated for 2 h with log-phase GBS at an MOI=1 or 0.1, after centrifugation at 1,600 rpm for 10 min to initiate cell contact. Cells were lysed with Triton X-100 (0.06 %), and surviving bacteria were quantified by serial dilution, plating, and enumeration. For supernatant antimicrobial activity, the supernatants were harvested after micrococcal nuclease treatment and were infected with GBS at 1×10^3 colony forming units (CFU)/ml. Surviving bacteria were quantified at 30 min by serial dilution, plating, and enumeration. ANOVA one-way analysis and Bonferroni's multiple comparison were used to analyze statistical significance.

Extracellular traps

Studies were performed as previously described [30]. In brief, Mϕs (3×10^5 cells/well) were incubated in 24-well plates with 300 μl RPMI 1640 with 2 % FBS. Mϕs were allowed to adhere for 2 h at 37 °C with 5 % CO_2, then stimulated with PMA (25 μM) or infected with live GBS for 60 min. To dissolve extracellular DNA traps, micrococcal nuclease was added at 1:500 for 20 min. Wells were rinsed three times with PBS, and extracellular traps were stained with Mammalian Dead staining (Invitrogen) for 10 min, followed by evaluation via fluorescent microscopy.

Flow cytometry

One million Mϕs were fixed in 1 % PFA and incubated with FITC-conjugated IL-10R Ab (1/200 dilution) for 60 min at 4 °C. Cells were analyzed using FACSort and CellQuest software (BD Biosciences).

Immunostaining

Mϕs (1×10^6) were grown on a sterile glass cover slide. Nonspecific binding was blocked by incubation with serum (20 %) from the host of secondary Ab and 0.2 % Tween 20 in PBS (0.5 h at 25 °C). Cells were incubated with primary Abs (1/200 dilution) for 1 h at 4 °C, extensively washed with PBS, and incubated with secondary Abs (1/1,000 dilution) for 0.5 h at 4 °C. Cells were fixed with 4 % paraformaldehyde (PFA) (10 min at 25 °C) and permeabilized with cold acetone (15 s). Nuclei were stained with 4′,6′-diamido-2-phenylindole (DAPI) hydrochloride (15 s at 25 °C), and cells were visualized using a fluorescent microscope.

Results

Activation of the SR results in faster phagosome maturation in murine Mϕs

We previously found that Mϕs exposed to HS or treated with geldanamycin increased their phagocytic capacity. This increase in phagocytosis was dependent on new gene expression [15]. However, the specific genes involved in this phenomenon have not yet been identified. In addition, actin polymerization was observed to increase upon SR activation in the absence of external or foreign stimuli [15, 16]. Formation of F-actin is a key element for the internalization of the newly formed phagosomes and also plays a role in their maturation [31]. These observations suggested that the SR might induce accelerated phagosome maturation. To assess phagosome maturation in stressed (42 °C, 1.5 h) and control J774 Mϕs, we measured co-localization of green phagosomes containing nonopsonized AF488-*E. coli* (green) and endosomes containing AF532-conjugated transferrin (red). We observed more rapid co-localization of phagosomes and endosomes (yellow and arrows) in stressed Mϕs (within 5 min) in comparison with control cells (7 min) as presented in Fig. 1a. In addition, the distribution of internalized *E. coli* particles was markedly different between control and stressed cells at 5 min of incubation. Thus, stressed cells showed a vesicular distribution of bacteria particles while control cells had a primarily peripheral distribution, supporting the data suggesting a faster internalization by stressed Mϕs. Faster formation of phagosomes was similarly observed when PMϕs were utilized (Fig. S1A).

S. aureus, opsonized bacteria particles, or latex beads (0.2 μm) were used, suggesting that this observation is independent of the ligand type or degree of opsonization. A rapid maturation of phagosomes could reflect accelerated internalization of bacteria, typically considered M1 ligands. Thus, we next evaluated the rate of internalization of IgG-opsonized BSA in J774 cells as well as in naïve PMϕs derived from BALB/c mice. We observed that stressed Mϕs display a faster internalization rate than nonstressed (control) Mϕs (Fig. 1b). It is important to remark that the same tendency (higher ratios of internalization) was observed before removing the noninternalized ligands by washes with acidified PBS, showing a 2.1-fold increase by stressed J744 cells and a 2.7-fold increase by stressed PMϕs derived from BALB/c mice, with respect to their controls. The ratios of IgG-opsonized BSA internalization were also measured in the presence of LPS (0.1 ng/ml), which displayed significantly higher internalization than observed in the absence of LPS (Fig. 1c), which suggests that the increase in internalization of IgG-opsonized BSA by HS Mϕs is not due to contamination with LPS. Interestingly, stressed cells also showed a faster endocytosis of transferrin (clathrin-mediated endocytosis) and cholera

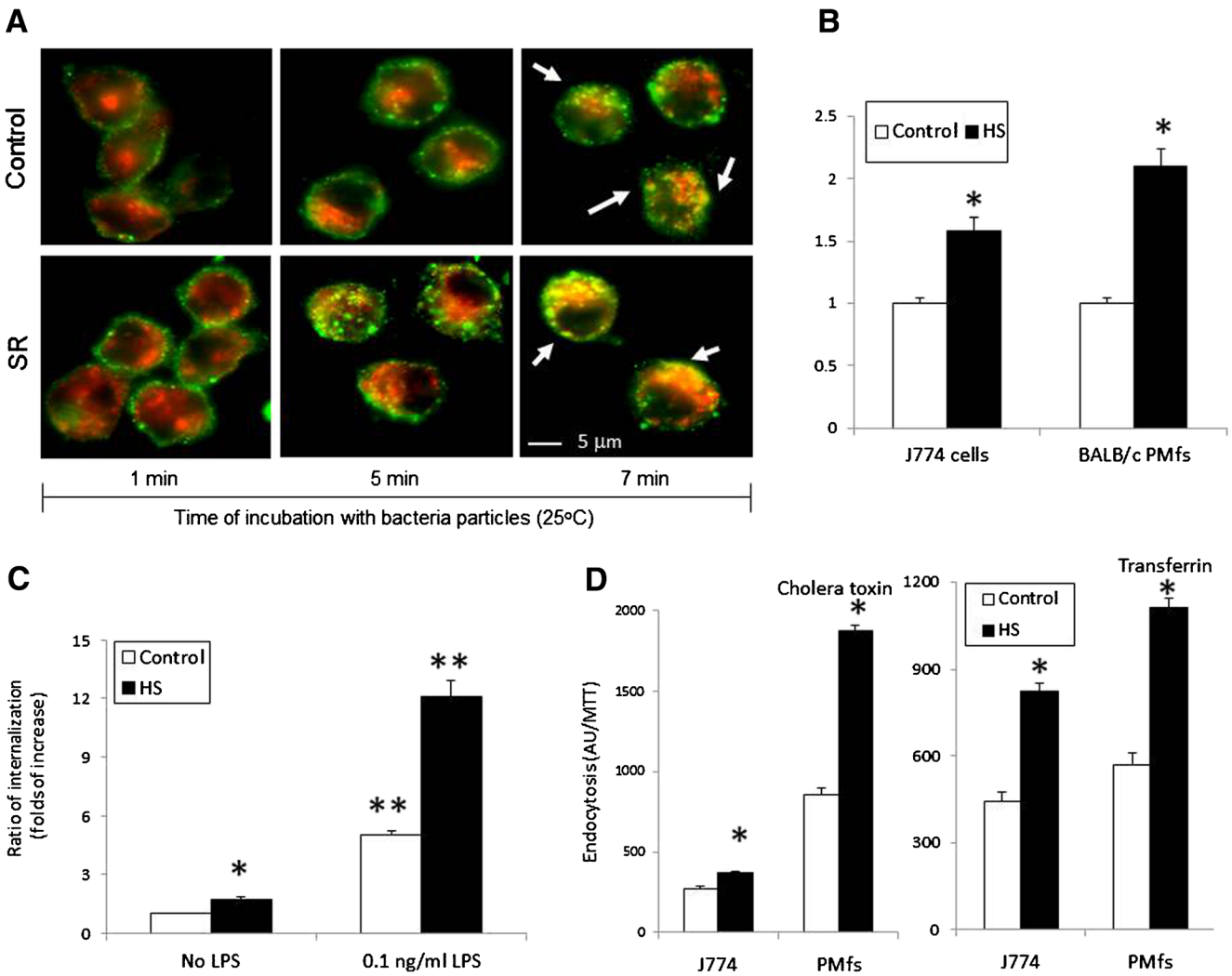

Fig. 1 Activation of the SR accelerates phagosome maturation and internalization of M1 ligands. **a** Phagosome maturation was evaluated in stressed and control cells by co-localization of AF532 transferrin-labeled endosomes (*red*) and AF488-conjugated bacteria particles (*green*). *Arrows* indicate co-localization of *red* and *green* (*yellow areas*). **b** Ratios of internalization of M1 ligand were measured using FITC-conjugated IgG-opsonized BSA by fluorometry using J774 cells and naïve PMϕs derived from BALB/c mice. HS cells were subjected to HS (42 °C, 1.5 h) and allowed to recover for 5 h. Noninternalized signal was removed by washing with SF media and membrane bound signal was removed by incubating with acidic PBS. Intensity of the signal was rectified by MTT values in each plate. **c** Internalization of FITC-conjugated IgG-opsonized BSA measured by fluorometry in the presence or absence of 0.1 ng/ml of LPS. **d** Endocytosis of transferrin (clathrin-mediated internalization) and cholera toxin (caveolin-1-mediated internalization) by control or stressed J774 cells or naïve PMϕs was quantified by incubating cells in SF medium for 30 min, followed by incubation with transferrin (5 μg/ml) or cholera toxin (5 μg/ml) for 30 min at 37 °C. Noninternalized signal was removed by washing with PBS. Internalized signal was rectified by MTT in each well. *$P<0.05$ with respect to control group; **$P<0.05$ with respect to HS group one-way ANOVA with Newman-Keuls post-tests

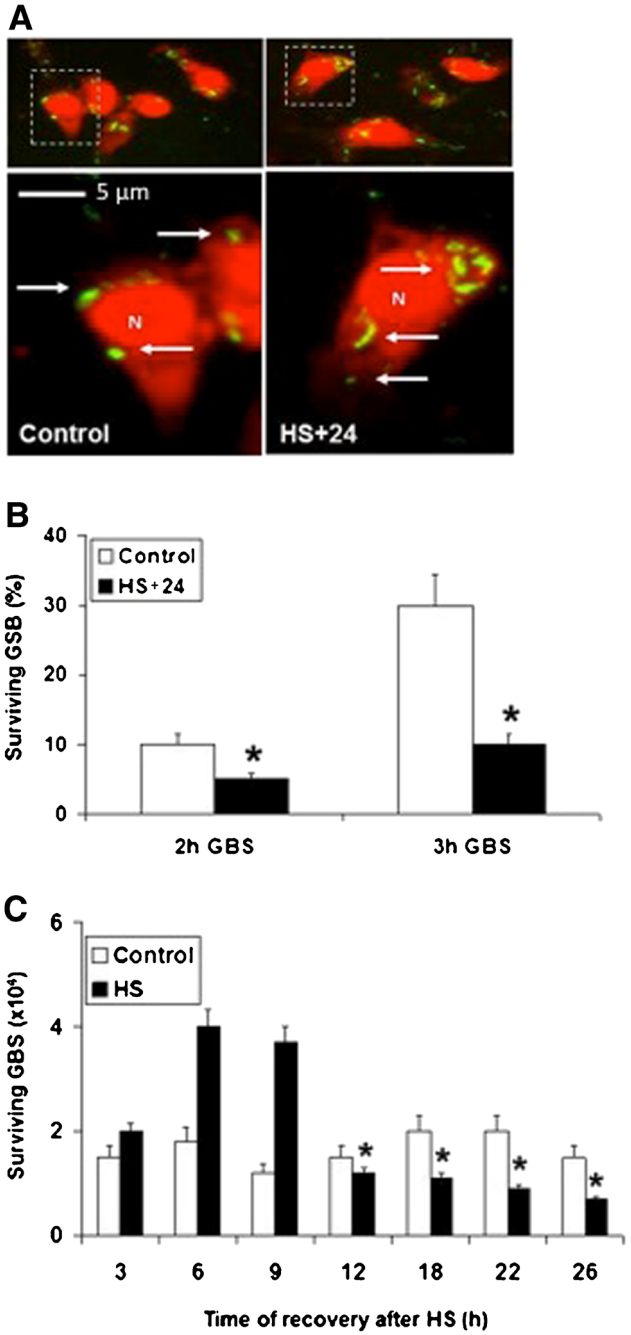

◀ **Fig. 2** Activation of SR increases Mϕ internalization and destruction of live GBS. Mϕs were subjected or not to HS (42 °C, 1.5 h) and allowed to recover for 24 h. Cells were infected with live GBS at an MOI of 10 (2 to 3 h at 37 °C). **a** Visualization of internalized live GBS-GFP by control and stressed (SR) cells. *Arrows* indicate the presence of internalized GBS-GFP within control or stressed cells. These experiments were performed at least three times, each in triplicate. **b** Increase in GBS killing activity by HS Mϕs was observed after 2 and 3 h of infection (MOI of 1). **P*<0.01; ***P*<0.001, by two-way ANOVA with Bonferroni post-tests. **c** Blocking phagocytosis via incubation of Mϕs with cytochalasin D (CytD, 50 µM for 30 min) decreased Mϕ killing of GBS. However, HS Mϕs maintain higher bactericidal activity compared to controls. **P*<0.01, with respect to control (non-HS) cells, by one-way ANOVA with Bonferroni post-tests. **d** Kinetics of increase in killing activity by HS Mϕs. Mϕs underwent HS and were allowed to recover for various amounts of time. Significant increases in killing activity were observed 12 h into the recovery time and persisted for up to 40 h (*data not shown*). **P*<0.01, with respect to control (non-HS) cells, by one-way ANOVA with Bonferroni post-tests

toxin (caveolin-1 endocytosis) as compared with nonstressed cells (Fig. 1d), suggesting that activation of the SR enhances internalization processes via a mechanism that is independent of the ligand or involved receptor.

Activation of the SR in Mϕs leads to increased killing capacity in response to GBS infection

Since stressed Mϕs have elevated phagocytosis and increased phagosome maturation rate, we next examined whether these properties translated into increased internalization and killing of bacteria (GBS-GFP). Mϕs subjected to HS (42 °C, 1.5 h) internalized significantly higher numbers of GBS-GFP when compared to nonstressed control cells (Fig. 2a, arrows). Similar differences were noted in the samples run without quenching of external, adherent bacteria, consistent with the differences seen being due to phagocytosis alone. Furthermore, Mϕs subjected to HS killed more bacteria than control cells (Fig. 2b). Blocking phagocytosis via incubation of Mϕs with cytochalasin D (CytD, inhibitor of actin polymerization) led to a dramatic reduction in both control and HS-linked bacterial killing. However, HS Mϕs maintained a modicum of bactericidal activity outside of phagocytic mechanisms (Fig. 2c). Kinetic analysis demonstrated that enhanced killing activity in stressed Mϕs becomes significantly higher than in control cells within 12 h and lasts up to 26 h into the recovery time (Fig. 2d). The cause of the decreased bacterial killing in the first 9h post-HS is likely due to the large amount of protein unfolding that is caused by HS and thus decreased cell functionality. Once heat shock proteins have completed their chaperone activities to reinstate correct protein folding, the cells regain functionality. This data suggests that while acute stress decreases the ability of Mϕs to clear pathogenic bacteria, the activation of the SR subsequently leads to overall improvement in Mϕ antimicrobial activities.

Enhanced killing capacity linked to SR activation is associated with enhanced formation of extracellular traps and increased expression of cathelicidin

In earlier studies, we had shown that increased killing activity by stressed cells was not due to the activation of membrane NADPH-oxidase during respiratory burst [25]. Thus, we evaluated the effect of the SR on other Mϕ killing mechanisms such as antibacterial DNA-based extracellular trap (ET) formation [32–36] and the expression of antimicrobial peptides

(AMPs). Mϕs were infected with live GBS bacteria and ET formation visualized by fluorescent microscopy. HS-treated Mϕs had increased ET formation at 60 min in response to GBS infection whereas control cells did not exhibit significant formation of these structures (Fig. 3a). All ET-producing Mϕs died within 3 h. However, 50 % of control cells were also dead secondary to infection with GBS. HS-triggered Mϕ ETs were functional and contributed to bacterial clearance and killing, as their disruption via treatment with micrococcal nuclease led to improved bacterial survival in HS cells alone (Fig. 3b).

Destruction of bacteria within ETs is associated with a framework of nuclear DNA in which histones, proteases, and AMPs are embedded [32, 37, 38]. Since AMPs serve a bactericidal role in ETs, we evaluated the induction of the murine cathelicidin-related AMP (CRAMP) in response to HS as well as to GBS infection in control and HS Mϕs. Activation of the SR alone resulted in a 2.3-fold increase in Mϕ CRAMP expression (measured by qRT-PCR) compared to control cells (Fig. 3c). Infection of stressed Mϕs with live GBS resulted in a further 3.5-fold increase in CRAMP expression (Fig. 3c), suggesting that cathelicidins play a role in the increased killing activity of HS Mϕs. To further evaluate this, supernatents were harvested from Mϕs after ET induction with PMA and breakdown with micrococcal nuclease. Supernatents from HS Mϕs stimulated with PMA to form ETs increased bactericidal activity compared to controls: 191 CFU surviving compared to 310 CFU in controls, 230 CFU in controls+PMA, and 230 CFU in HS supernatent alone (P=0.0188, one-way ANOVA with Bonferroni post-tests). This data supports the increased production and release of antimicrobial factors by HS Mϕs, via secretion as well as being embedded within ETs.

Another bactericidal mechanism of Mϕs is the release of nitric oxide (NO), which is produced by a reaction catalyzed by inducible nitric oxide synthase (iNOS). The expression of

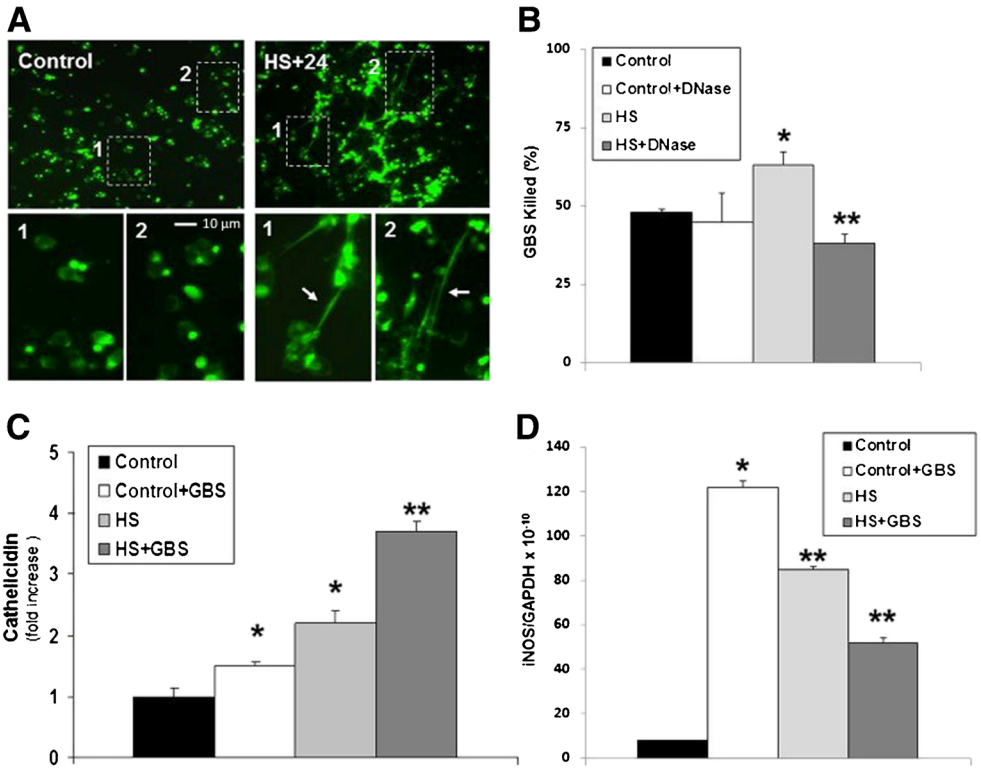

Fig. 3 Activation of the SR triggers an increase in bactericidal activity, which is linked to ET formation and enhanced expression of cathelicidin. Mϕs were subjected or not to HS (42 °C, 1.5 h) and allowed to recover for 24 h at 37 °C. **a** Mϕs were infected with live GBS (MOI of 1) for 1 h and then stained with Mammalian Live/Dead stain to visualize ETs under fluorescent microscopy. *Arrows* indicate the presence of ETs after incubation with live GBS and were found exclusively in HS-treated cells. **b** Improved bactericidal function of stressed cells is abolished by disruption of ETs. Treatment of HS Mϕs with DNase prior to GBS infection resulted in the disruption of ETs as well as a significant decrease in GBS killing capacity in stressed cells. DNase treatment had no effect on the killing capacity of control cells. *P<0.01 with respect to control or untreated cells; **P<0.001 with respect to HS cells, one-way ANOVA with Bonferroni post-tests. **c** Expression of cathelicidin was measured by qRT-PCR using commercially available primers. *P<0.01, with respect to control or untreated cells; **P<0.01 with respect to control Mϕs in the presence or absence of GBS as well as heat-shocked cells. **d** Expression of iNOS was measured by qRT-PCR in control and stressed cells in the presence or absence of GBS (MOI of 1 for 1 h). Values were rectified by GAPDH. *P<0.05, with respect to control; **P<0.05, with respect to control cells infected with GBS, analyzed via one-way ANOVA with Newman-Keuls post-tests

iNOS at the level of messenger RNA (mRNA) was significantly reduced when cells were subjected to HS and then stimulated with live GBS (Fig. 3d). In addition, the production of nitrites, measured by the Griess reaction, was also reduced in stressed cells stimulated with live GBS (46.9 μM/MTT), in clear contrast with nonstressed control cells stimulated with live GBS (74.6 μM/MTT). Thus, SR activation induces ET formation and increases cathelicidin expression, which contribute to enhanced bactericidal activities of HS Mϕs. However, the SR also decreases iNOS expression and the production of nitrites.

Activation of the SR decreases pro-inflammatory cytokine expression in response to M1 ligands

To characterize the role of SR activation on M1/M2 phenotype balance in Mϕs, we measured the expression of TNF-α and IL-6 in control or HS Mϕs in the presence and absence of live GBS, an M1 stimulus. HS by itself did not trigger the expression of TNF-α (Fig. 4a). Moreover, stressed cells expressed significantly lower amounts of TNF-α in response to live GBS infection as compared to nonstressed control cells (Fig. 4b). Measurements of extracellular levels of TNF-α by ELISA showed no differences between control and stressed

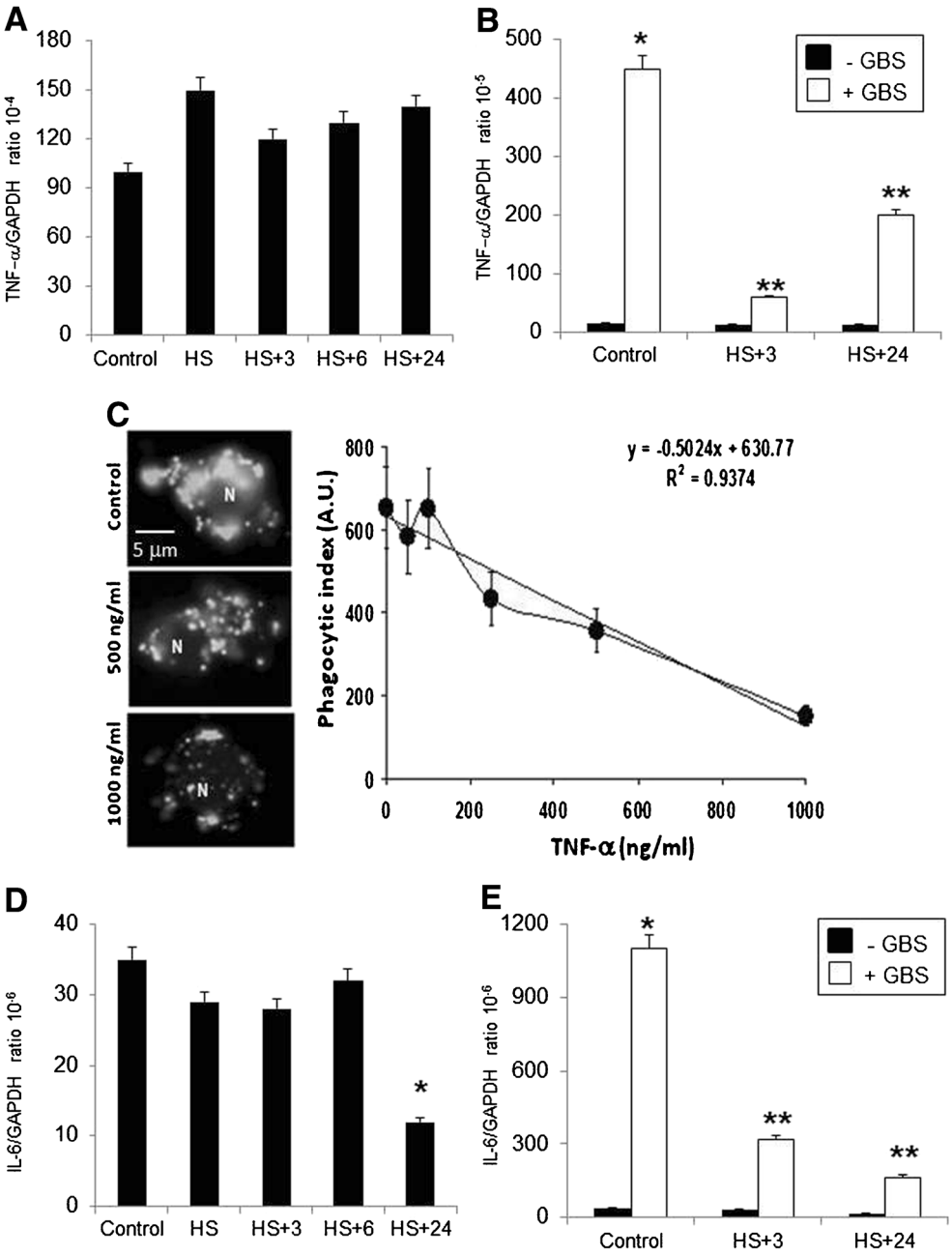

Fig. 4 Decreased expression of TNF-α and IL-6 in response to GBS is observed in stressed Mϕs. J774 cells were subjected or not to HS (42 °C for 1.5 h) and then allowed to recover for different lengths of time up to 24 h. Levels of TNF-α (**a**, **b**) and IL-6 (**d**, **e**) mRNA were evaluated by qRT-PCR in stressed and nonstimulated (control) Mϕs in the presence or absence of live GBS (MOI 1, 1 h). Values were rectified by GAPDH. Data was analyzed by one-way ANOVA followed by Newman-Keuls test. *$P<0.01$ with respect to control cells (no GBS). **$P<0.01$ with respect to control cells infected or not with GBS. **c** J774 cells were incubated with increasing concentrations of recombinant murine TNF-α for 24 h, followed by assessment of phagocytosis of bacterial particles. Phagocytosis decreased in response to increasing concentrations of rTNF-α, in a dose-dependent manner. Results were rectified by MMT in each well and results are expressed as phagocytic index (A.U.)

cells (10.1 pg/ml/MTT in nonstressed controls versus 12.4 pg/ml/MTT after HS and 3 h recovery or 9.9 pg/ml/MTT after HS and 24 h recovery). On the contrary, a significant reduction in live GBS-induced TNF-α levels was observed in stressed cells (HS+3, 235.7 pg/ml/MTT and HS+24, 467.8 pg/ml/MTT) as compared with nonstressed control cells (3,451.3 pg/ml/MTT). Similar data was found when AMϕs and PMϕs derived from naïve BALB/c mice were infected with live GBS (Fig. S1A). This decreased expression of TNF-α could be part of the mechanism responsible for the increased phagocytosis by stressed Mϕs because we have observed that internalization of bacteria particles is inversely proportional, in a concentration-dependent manner, to exogenous addition of recombinant murine TNF-α (Fig. 4c). Similarly, IL-6 expression was not influenced by HS alone (Fig. 4d), and the combination of HS and GBS infection also resulted in lower expression of this cytokine when compared to infected nonstressed control cells (Fig. 4e, S1B). Similar results were observed by using PMϕs or AMϕs derived from naïve BALB/c mice exposed to GBS (Fig. S1B). We also observed decreased expression of the IL-23 p40 subunit upon SR activation, while expression levels of the IL-23 p19 subunit, IL-17, IL-12 p35 subunit, and TGF-β were unchanged (Fig. S2). These data suggest that activation of the SR significantly modifies the expression of certain pro-inflammatory mediators (i.e., TNF-α and IL-6) in

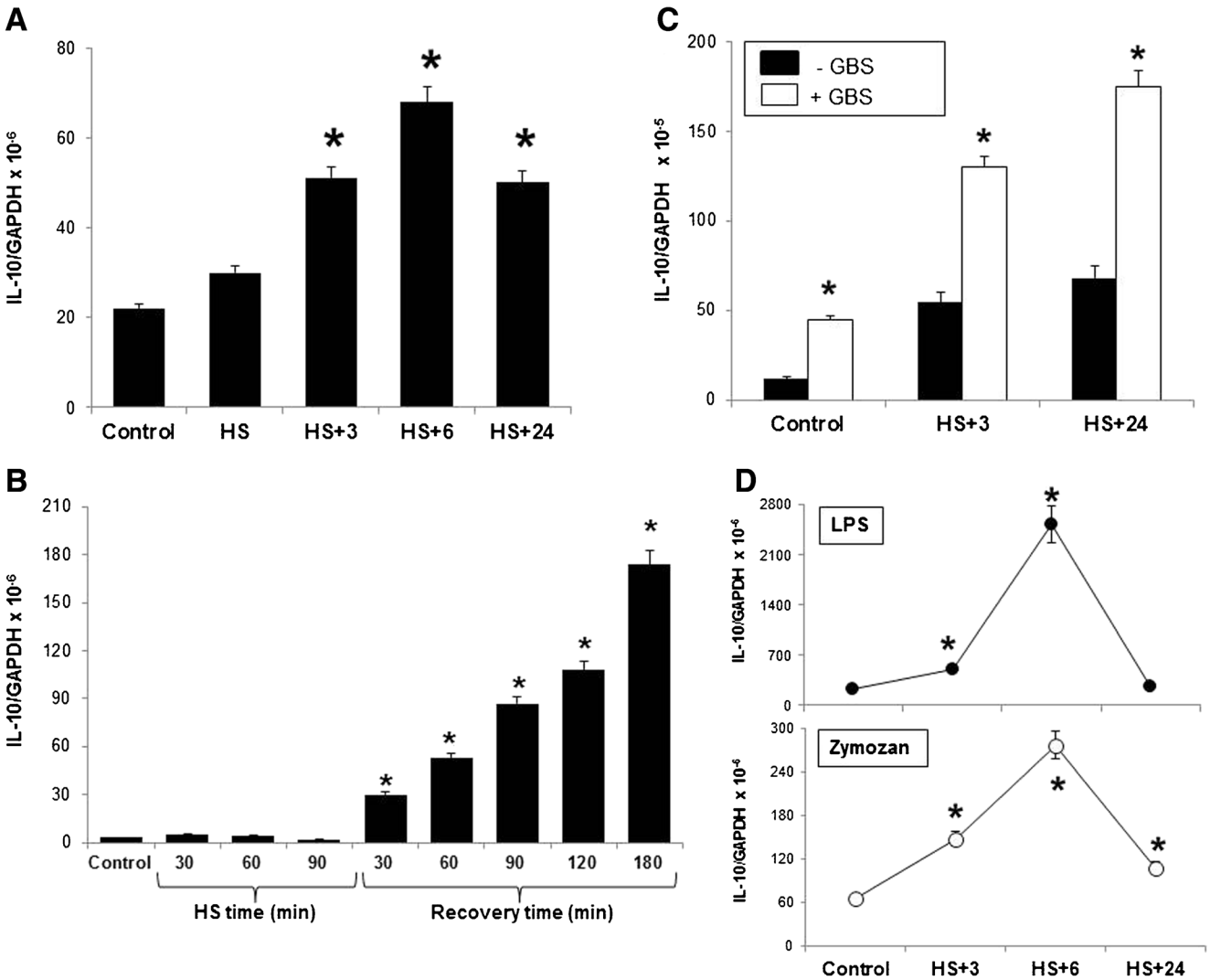

Fig. 5 SR strongly induces IL-10 expression in vitro. J774 cells (1×10^6 cells per well) were subjected or not to HS (42 °C for 1.5 h) and then allowed to recover for 3, 6, and 24 h. IL-10 mRNA levels were quantified by qRT-PCR in nonstimulated (control) and stressed cells and rectified by GAPDH expression in each sample. **a** HS increased expression of IL-10 in the absence of M1 ligand, with peak levels at 6 h into recovery. **b** HS-associated increase in IL-10 expression started at 30 min into the recovery time. **c** Infection of heat stressed cells with live GBS resulted in a synergistic effect on IL-10 production. **d** Synergistic increases in IL-10 levels were also observed when stressed Mϕs were incubated with other M1 ligands such as LPS (100 ng/ml for 1 h) and zymozan (200 μg/ml for 1 h). Data was analyzed by one-way ANOVA followed by Newman-Keuls test. *$P<0.01$ with respect to control cells

response to GBS infection, which is an M1 stimulus. These results were confirmed using other M1 ligands, such as lipopolysaccharide (LPS), zymozan, and bacteria particles (Fig. S3).

Enhanced expression of IL-10 and mrc-1 by stressed Mϕs in the presence or absence of GBS

It is well known that levels of TNF-α are inversely proportional to the concentration of IL-10 [39, 40]. Thus, we decided to investigate the effect of SR activation on the expression of IL-10. We observed an induction of IL-10 mRNA after HS in the absence of M1 ligand stimulation (Fig. 5a), suggesting that expression of this anti-inflammatory cytokine is strongly modulated by the thermal stress. Interestingly, the enhancement in IL-10 expression begins early in recovery (30 min; Fig. 5b), which may suggest a specific role of IL-10 in the development of the SR-linked phenotypes. Infection of stressed cells with live GBS resulted in a synergistic elevation of IL-10 expression (Fig. 5c). Other Mϕ activators such as zymozan, IgG-opsonized bacteria particles, and LPS showed similar synergy with HS (Fig. 5d). We did not observe changes in IL-10 receptor (FITC-labeled) levels after HS, as demonstrated by flow cytometry (Fig. 6a). In contrast, increased translocation of STAT3 into the nucleus was observed in response to M1 ligand in stressed Mϕs as opposed to stressed cells in absence of LPS or nonstressed cells without an external stimulus (Fig. 6b). These results suggest that the IL-10 signal transduction pathways are stimulated in stressed Mϕs, and they may contribute to formation of an intermediary

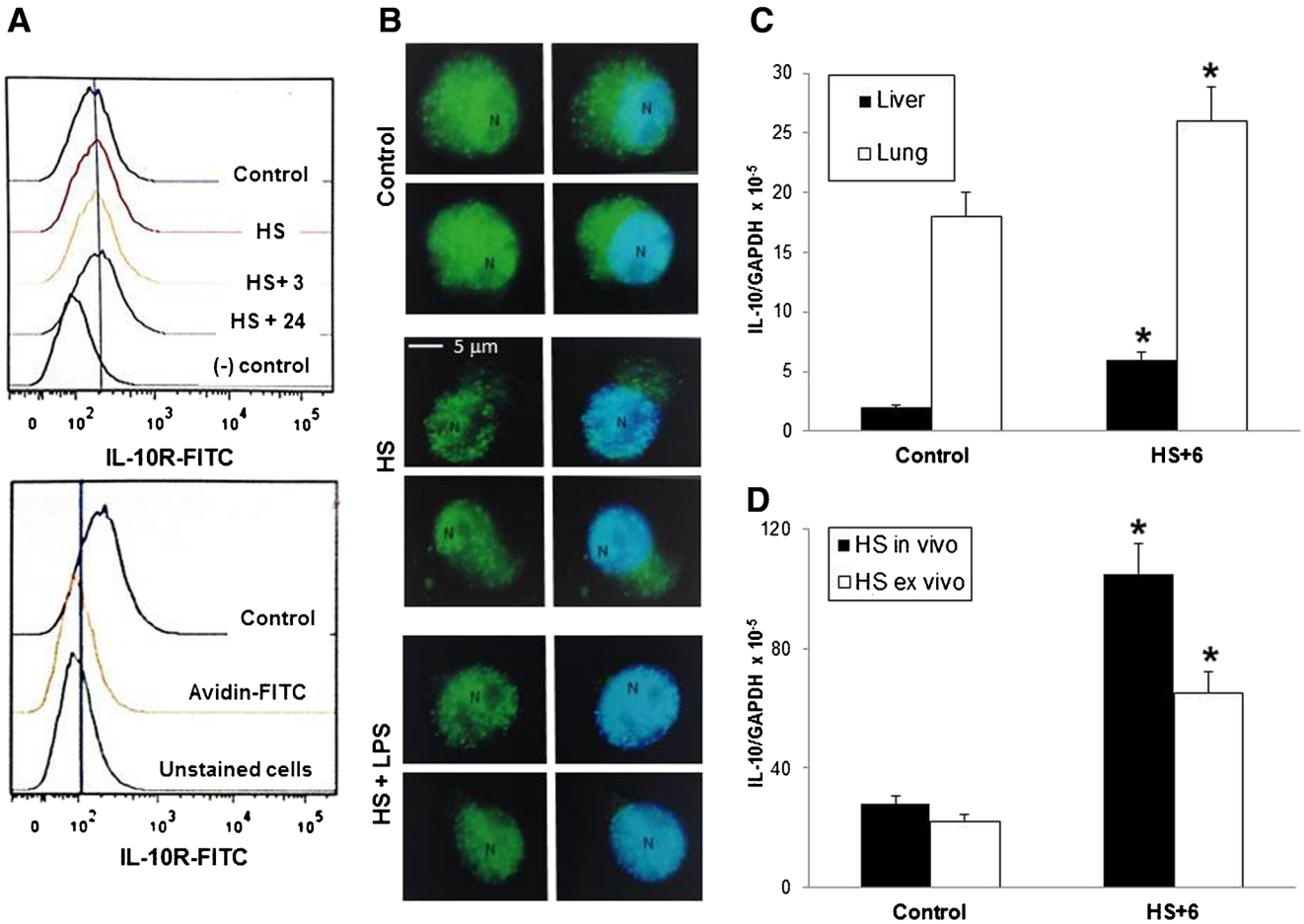

Fig. 6 IL-10R levels are not modified by SR activation while STAT3 translocation into the nucleus is increased in stressed Mϕs. **a** Levels of IL-10R on the cell surface of control or stressed Mϕs were measured by FACs analysis using a commercially available kit (anti-IL-10R-FITC antibody). No changes in the quantity of IL-10R bound by the antibody were observed when control and HS cells were compared. **b** HS alone or in combination with LPS, an M1 ligand, resulted in translocation of STAT3 (*green*) into the nuclei (*blue*). As expected, STAT3 translocation into the nucleus was maximal when both conditions were present (HS+ LPS), with almost no STAT3 remaining in the cytoplasm, which may be linked to the higher levels of IL-10 produced. **c** Induction of HS in vivo also resulted in the upregulation of IL-10 expression. In brief, BALB/c male mice (8 weeks old) were subjected to HS as described in Paidas et al. [33]. Mice were allowed to recover for 6 h after HS and then liver, lung, and PMϕs were isolated. Macrophages that underwent HS in vivo behave similarly to macrophages in which HS was induced ex vivo (**d**). Data was analyzed by one-way ANOVA followed by Newman-Keuls test. *$P<0.01$ with respect to control cells or non-HS mice

Mϕ phenotype in which anti-inflammatory and antibacterial activities are enhanced.

We also found that the expression of IL-10 was significantly higher in the lung and liver derived from mice subjected to HS and recovered for 6 h at normal temperatures as compared with non-HS control mice (Fig. 6c). These results are consistent with prior reports indicating increased production of IL-10 and lower production of TNF-α in vivo when male BALB/c mice were subjected to thermal stress [27]. In addition, isolation of PMϕs from control and HS mice showed the same cytokine profile described above: low expression of TNF-α (data not shown) and elevated expression of IL-10. The elevation in IL-10 from in vivo HS PMϕs was similar to that of PMϕs isolated from control mice and then exposed to HS ex vivo (Fig. 6d).

Finally, we investigated other well known markers of Mϕ polarization and discovered that the M2-associated gene mrc-1 had increased expression in response to HS (Fig. S4A) [7]. Control Mϕs infected with GBS respond with increased expression of ptgs-2, a classic M1 marker [41], and decreased mrc-1 and ym-1, M2 markers (Fig. S4B) [42]. HS Mϕs infected with GBS have further increased expression of mrc-1 (Fig. S4C). These data further characterize HS Mϕs as having anti-inflammatory (increased IL-10 with decreased TNF-α and IL-6) and anti-bacterial (increased ETs and CRAMP expression) functional characteristics as well as M2 (mrc-1) characteristics. Overall, our data describe a unique Mϕ activation and functional type within an ever growing spectrum of Mϕ phenotypes.

Discussion

Hsp70 expression is increased after stress, either by treatment with geldanamycin or by HS [15], which has been linked to improving internalization of several ligands, including transferrin, cholera toxin [16], and opsonized particles [17]. It is also possible that expression of Hsp70 plays a role in phenotypic changes of Mϕs. The involvement of Hsp expression, in particular Hsp70, in Mϕ function was supported by the time-dependent increase in bacterial killing capacity presented in the current study. The expression of Hsps immediately after the initial thermal injury is mainly targeted to the refolding of polypeptides that are damaged during the insult, preventing their degradation. As time passes and fewer damaged proteins are present, Hsps may play unconventional/nontraditional roles such as modulating killing capacity and ET formation. This hypothesis is supported by the fact that HS effects on these innate immune phenotypes last up to 26 h after thermal stress, whereas levels of misfolded or damaged proteins return to physiological levels within 9 h [27].

In this study, we observed the lack of significant ROS or RNS production by stressed Mϕs, which was compensated by the significant activation of other bactericidal mechanisms, including ET formation and expression of cathelicidin antimicrobial peptide (CAMP). ETs are genomic DNA-based net-like structures that capture bacteria and fungi. The formation of ETs is promoted by increased production of ROS and pro-inflammatory mediators such as TNF-α and IL-1β, while IL-10, per se, tends to inhibit these structures from being formed [43, 44]. Thus, these are unlikely to be the mechanisms involved with SR-associated induction of ETs, since we report in this study a decreased expression of pro-inflammatory mediators but elevated levels of IL-10. On the contrary, we speculate that changes in the cytoskeleton triggered by SR activation, such as enhanced formation of F-actin [15], are responsible for ET formation in the absence of oxidative stress or severe inflammation. Participation of actin and tubulin in ET formation has been previously reported [45]. The mechanisms by which the SR triggers cytoskeleton changes remain unknown, although expression of Hsp70 and Hsp27 may play a role.

AMPs, which are 12–100 amino acid peptides, have been shown to play a critical role in innate immunity due to their anti-bactericidal capacities [46]. Expression of AMPs can be constitutive or can be inducible by infectious and/or pro-inflammatory stimuli, such cytokines, bacteria, or bacterial molecules [47, 48]. Our data demonstrates that stressed Mϕs, in the absence of pathogens, express higher levels of cathelicidin, which increases further when infected with live GBS. The increased levels of cathelicidin likely contribute to bacterial killing and thus clearance of noxious stimuli.

Conclusions

Activation of the SR modulates polarity in stressed Mϕs by promoting an M2-like production of anti-inflammatory signals (IL-10) and gene expression (mrc-1), while also promoting M1-like killing of pathogens via increased phagocytosis, AMP production, and ET formation. This “friendly activation” helps Mϕs fight bacterial infections while trying to protect tissues from damage caused by excessive inflammation, such as that observed in sepsis. Elucidation of SR-related mechanisms that control the balance of Mϕ functional polarity may have enormous potential applications in the treatment or prevention of diseases where the Mϕ polarity is inappropriate.

Acknowledgments We thank Molly Wofford for her editorial assistance. We thank Elisa McEachern and Matthew Lyes for their intellectual and experimental contributions. This work was supported through a Veterans Affairs Career Development Award (CDA)-2, BX-10-014 (PI, Laura E. Crotty Alexander), The Hartwell Foundation Biomedical Research Fellowship (Laura E. Crotty Alexander), University of California San Diego Academic Senate Grant (PI, Virginia L. Vega), and GM R01 098455 and GM R25 083275 grants (PI, Antonio De Maio).

Conflict of interest The authors have no financial conflicts of interest.

Authors' contribution LECA, VLV, and JHW designed all of the experiments. LECA, VLV, WC, and JHW ran all of the experiments. LECA, VLV, JHW, VN, and ADM analyzed and interpreted all of the data and wrote the manuscript.

References

1. Liu G, Yang H (2013) Modulation of macrophage activation and programming in immunity. J Cell Physiol 228:502–512
2. Busse W, Corren J, Lanier BQ, McAlary M, Fowler-Taylor A, Cioppa GD, van As A, Gupta N (2001) Omalizumab, anti-IgE recombinant humanized monoclonal antibody, for the treatment of severe allergic asthma. J Allergy Clin Immunol 108:184–190
3. van Dullemen HM, van Deventer SJ, Hommes DW, Bijl HA, Jansen J, Tytgat GN, Woody J (1995) Treatment of Crohn's disease with anti-tumor necrosis factor chimeric monoclonal antibody (cA2). Gastroenterology 109:129–135
4. Cohen SB, Emery P, Greenwald MW, Dougados M, Furie RA, Genovese MC, Keystone EC, Loveless JE, Burmester GR, Cravets MW et al (2006) Rituximab for rheumatoid arthritis refractory to anti-tumor necrosis factor therapy: results of a multicenter, randomized, double-blind, placebo-controlled, phase III trial evaluating primary efficacy and safety at twenty-four weeks. Arthritis Rheum 54:2793–2806
5. Biswas SK, Mantovani A (2010) Macrophage plasticity and interaction with lymphocyte subsets: cancer as a paradigm. Nat Immunol 11:889–896
6. Mosser DM, Edwards JP (2008) Exploring the full spectrum of macrophage activation. Nat Rev Immunol 8:958–969
7. Gordon S (2003) Alternative activation of macrophages. Nat Rev Immunol 3:23–35
8. Mantovani A, Sica A, Sozzani S, Allavena P, Vecchi A, Locati M (2004) The chemokine system in diverse forms of macrophage activation and polarization. Trends Immunol 25:677–686
9. Mantovani A, Sozzani S, Locati M, Schioppa T, Saccani A, Allavena P, Sica A (2004) Infiltration of tumours by macrophages and dendritic cells: tumour-associated macrophages as a paradigm for polarized M2 mononuclear phagocytes. Novartis Found Symp 256:137–145, discussion 146–138, 259–169
10. Li J, Hsu HC, Mountz JD (2012) Managing macrophages in rheumatoid arthritis by reform or removal. Curr Rheumatol Rep 14:445–454
11. Liu C, Li Y, Yu J, Feng L, Hou S, Liu Y, Guo M, Xie Y, Meng J, Zhang H et al (2013) Targeting the shift from m1 to m2 macrophages in experimental autoimmune encephalomyelitis mice treated with fasudil. PLoS One 8:e54841
12. Nazari-Jahantigh M, Wei Y, Noels H, Akhtar S, Zhou Z, Koenen RR, Heyll K, Gremse F, Kiessling F, Grommes J et al (2012) MicroRNA-155 promotes atherosclerosis by repressing Bcl6 in macrophages. J Clin Invest 122:4190–4202
13. Laskin DL, Pendino KJ (1995) Macrophages and inflammatory mediators in tissue injury. Annu Rev Pharmacol Toxicol 35:655–677
14. Currie AJ, Curtis S, Strunk T, Riley K, Liyanage K, Prescott S, Doherty D, Simmer K, Richmond P, Burgner D (2011) Preterm infants have deficient monocyte and lymphocyte cytokine responses to group B streptococcus. Infect Immun 79:1588–1596
15. Vega VL, De Maio A (2005) Increase in phagocytosis after geldanamycin treatment or heat shock: role of heat shock proteins. J Immunol 175:5280–5287
16. Vega VL, Charles W, De Maio A (2010) A new feature of the stress response: increase in endocytosis mediated by Hsp70. Cell Stress Chaperones 15:517–527
17. Vega VL, Rodriguez-Silva M, Frey T, Gehrmann M, Diaz JC, Steinem C, Multhoff G, Arispe N, De Maio A (2008) Hsp70 translocates into the plasma membrane after stress and is released into the extracellular environment in a membrane-associated form that activates macrophages. J Immunol 180:4299–4307
18. Green SA, Kelly RB (1990) Endocytic membrane traffic to the Golgi apparatus in a regulated secretory cell line. J Biol Chem 265:21269–21278
19. Flesch IE, Kaufmann SH (1991) Mechanisms involved in mycobacterial growth inhibition by gamma interferon-activated bone marrow macrophages: role of reactive nitrogen intermediates. Infect Immun 59:3213–3218
20. Maridonneau-Parini I, Malawista SE, Stubbe H, Russo-Marie F, Polla BS (1993) Heat shock in human neutrophils: superoxide generation is inhibited by a mechanism distinct from heat-denaturation of NADPH oxidase and is protected by heat shock proteins in thermotolerant cells. J Cell Physiol 156:204–211
21. Souren JE, Van Der Mast C, Van Wijk R (1997) NADPH-oxidase-dependent superoxide production by myocyte-derived H9c2 cells: influence of ischemia, heat shock, cycloheximide and cytochalasin D. J Mol Cell Cardiol 29:2803–2812
22. Maridonneau-Parini I, Clerc J, Polla BS (1988) Heat shock inhibits NADPH oxidase in human neutrophils. Biochem Biophys Res Commun 154:179–186
23. Glaser P, Rusniok C, Buchrieser C, Chevalier F, Frangeul L, Msadek T, Zouine M, Couve E, Lalioui L, Poyart C et al (2002) Genome sequence of *Streptococcus agalactiae*, a pathogen causing invasive neonatal disease. Mol Microbiol 45:1499–1513
24. Vega VL, De Cabo R, De Maio A (2004) Age and caloric restriction diets are confounding factors that modify the response to lipopolysaccharide by peritoneal macrophages in C57BL/6 mice. Shock 22:248–253
25. Vega VL, Charles W, Crotty Alexander LE (2011) Rescuing of deficient killing and phagocytic activities of macrophages derived from non-obese diabetic mice by treatment with geldanamycin or heat shock: potential clinical implications. Cell Stress Chaperones 16:573–581
26. Crotty Alexander LE, Akong-Moore K, Feldstein S, Johansson P, Nguyen A, McEachern EK, Nicatia S, Cowburn AS, Olson J, Cho JY et al (2013) Myeloid cell HIF-1alpha regulates asthma airway resistance and eosinophil function. J Mol Med 91:637–644
27. Paidas CN, Mooney ML, Theodorakis NG, De Maio A (2002) Accelerated recovery after endotoxic challenge in heat shock-pretreated mice. Am J Physiol Regul Integr Comp Physiol 282:R1374–1381
28. Cramer T, Yamanishi Y, Clausen BE, Forster I, Pawlinski R, Mackman N, Haase VH, Jaenisch R, Corr M, Nizet V et al (2003) HIF-1alpha is essential for myeloid cell-mediated inflammation. Cell 112:645–657
29. Chow CW, Downey GP, Grinstein S (2004) Measurements of phagocytosis and phagosomal maturation. Current protocols in cell biology. 22:15.7:15.7.1–15.7.33
30. Crotty Alexander LE, Maisey HC, Timmer AM, Rooijakkers SH, Gallo RL, von Kockritz-Blickwede M, Nizet V (2010) M1T1 group A streptococcal pili promote epithelial colonization but diminish systemic virulence through neutrophil extracellular entrapment. J Mol Med 88:371–381
31. Liebl D, Griffiths G (2009) Transient assembly of F-actin by phagosomes delays phagosome fusion with lysosomes in cargo-overloaded macrophages. J Cell Sci 122:2935–2945
32. Chow OA, von Kockritz-Blickwede M, Bright AT, Hensler ME, Zinkernagel AS, Cogen AL, Gallo RL, Monestier M, Wang Y, Glass CK et al (2010) Statins enhance formation of phagocyte extracellular traps. Cell Host Microbe 8:445–454

33. Aulik NA, Hellenbrand KM, Czuprynski CJ (2012) Mannheimia haemolytica and its leukotoxin cause macrophage extracellular trap formation by bovine macrophages. Infect Immun 80:1923–1933
34. Mohanan S, Horibata S, McElwee JL, Dannenberg AJ, Coonrod SA (2013) Identification of macrophage extracellular trap-like structures in mammary gland adipose tissue: a preliminary study. Front Immunol 4:67
35. Wong KW, Jacobs WR Jr (2013) Mycobacterium tuberculosis exploits human interferon gamma to stimulate macrophage extracellular trap formation and necrosis. J Infect Dis 208:109–119
36. Hellenbrand KM, Forsythe KM, Rivera-Rivas JJ, Czuprynski CJ, Aulik NA (2013) Histophilus somni causes extracellular trap formation by bovine neutrophils and macrophages. Microb Pathog 54:67–75
37. Goldmann O, Medina E (2012) The expanding world of extracellular traps: not only neutrophils but much more. Front Immunol 3:420
38. von Kockritz-Blickwede M, Nizet V (2009) Innate immunity turned inside-out: antimicrobial defense by phagocyte extracellular traps. J Mol Med 87:775–783
39. Murray PJ (2006) Understanding and exploiting the endogenous interleukin-10/STAT3-mediated anti-inflammatory response. Curr Opin Pharmacol 6:379–386
40. Murray PJ (2005) The primary mechanism of the IL-10-regulated antiinflammatory response is to selectively inhibit transcription. Proc Natl Acad Sci U S A 102:8686–8691
41. Nakanishi Y, Nakatsuji M, Seno H, Ishizu S, Akitake-Kawano R, Kanda K, Ueo T, Komekado H, Kawada M, Minami M et al (2011) COX-2 inhibition alters the phenotype of tumor-associated macrophages from M2 to M1 in ApcMin/+mouse polyps. Carcinogenesis 32:1333–1339
42. Nair MG, Cochrane DW, Allen JE (2003) Macrophages in chronic type 2 inflammation have a novel phenotype characterized by the abundant expression of Ym1 and Fizz1 that can be partly replicated in vitro. Immunol Lett 85:173–180
43. Keshari RS, Jyoti A, Dubey M, Kothari N, Kohli M, Bogra J, Barthwal MK, Dikshit M (2012) Cytokines induced neutrophil extracellular traps formation: implication for the inflammatory disease condition. PLoS One 7:e48111
44. Saitoh T, Komano J, Saitoh Y, Misawa T, Takahama M, Kozaki T, Uehata T, Iwasaki H, Omori H, Yamaoka S et al (2012) Neutrophil extracellular traps mediate a host defense response to human immunodeficiency virus-1. Cell Host Microbe 12:109–116
45. Neeli I, Dwivedi N, Khan S, Radic M (2009) Regulation of extracellular chromatin release from neutrophils. J Innate Immun 1:194–201
46. Zasloff M (2002) Antimicrobial peptides of multicellular organisms. Nature 415:389–395
47. Cunliffe RN, Mahida YR (2004) Expression and regulation of antimicrobial peptides in the gastrointestinal tract. J Leukoc Biol 75:49–58
48. Hancock RE (2001) Cationic peptides: effectors in innate immunity and novel antimicrobials. Lancet Infect Dis 1:156–164